



# A comparative study on thermal decomposition behavior of biodiesel samples produced from shea butter over micro- and mesoporous ZSM-5 zeolites using different kinetic models

Peter Adeniyi Alaba<sup>1</sup> · Yahaya Muhammad Sani<sup>2</sup> · Wan Mohd Ashri Wan Daud<sup>1</sup>

Received: 29 November 2015 / Accepted: 25 April 2016  
© Akadémiai Kiadó, Budapest, Hungary 2016

**Abstract** This study compared the kinetics of biodiesel produced over mesoporous ZSM-5 zeolites (0.3mesoZBio and 0.4mesoZBio) and conventional ZSM-5 zeolites (ZBio). The pyrolysis of each biodiesel was carried out in the presence of nitrogen at different heating rates of 10, 15 and 20 °C min<sup>-1</sup>. The reaction order, activation energy ( $E_A$ ) and frequency factor ( $A$ ) were computed using four different models. The models are Arrhenius, Coats–Redfern, Ingraham–Marrier and Differential model. According to the computed average activation energy based on first order, the activation energies of the produced biodiesel are very close. ZBio exhibits the highest  $E_A$  (86.53 kJ mol<sup>-1</sup>) compared to 0.3mesoZBio and 0.4mesoZBio (84.92 and 83.26 kJ mol<sup>-1</sup>, respectively). Therefore, it is tenable to adduce ZBio as the most stable because higher activation energy engenders higher stability.

**Keywords** Kinetic · Pyrolysis · Mesoporous ZSM-5 · Biodiesel · Shea butter

## Introduction

Demand for sustainable production of biodiesel as an alternative energy source is ever increasing. This is because of their environmental friendliness, acceptable quality of exhaust gasses and similarity to petroleum diesel [1]. This

demand arises from the need to minimize the use of fossil fuel by replacement with a suitable alternative energy source that is renewable and sustainable. This effort is being accelerated by depletion of fossil fuel reserve, ever-increasing fuel price and environmental pollution via greenhouse gas (GHG) emission [2]. Therefore, there arises a need to find fuel processing techniques that could help to obtain quality fuel products. Biodiesel is an essential renewable and sustainable energy source of this repute.

Shea butter is an extract of shea nut cheaply obtained from sub-Saharan African shea tree (*Vitellaria paradoxa*). It is an ivory-colored fat with high free fatty acid (FFA) content [3, 4]. The FFA contents are mainly of steric and oleic acid. Shea butter enjoyed wide utilization in confectionery and cosmetic industry; however, the use of shea butter in biodiesel production is still under investigation. The previous work on the transformation of shea butter to biodiesel was done via homogeneous catalysis [5–7]. The properties of crude shea butter are presented in Table 1.

Pyrolysis kinetics of biodiesel is of vital importance in thermochemical transformation process for energy production [8]. Pyrolysis is a thermochemical treatment that culminates in decomposition of organic materials at an elevated temperature in an oxygen- or any halogen-free environment [9–11]. As it proceeds, the physical and chemical phases of the materials are transformed irreversibly. Pyrolysis kinetics helps to model thermochemical conversion of biomass to biodiesel. Pyrolysis breaks the molecules to volatiles and residue. Pyrolysis kinetics is very complex because biofuel decomposition, yield and composition are influenced by many parameters. This includes moisture content, temperature, heating rate, resident time, size biofuel composition and particles [12–14]. Thermogravimetric analysis (TG) is a useful tool for evaluation of thermal decomposition because of its

✉ Wan Mohd Ashri Wan Daud  
ashri@um.edu.my

<sup>1</sup> Department of Chemical Engineering, University of Malaya, 50603 Kuala Lumpur, Malaysia

<sup>2</sup> Department of Chemical Engineering, Ahmadu Bello University, Zaria 870001, Nigeria

**Table 1** Properties of crude shea butter [4]

Properties	Values
Density/kg m <sup>-3</sup> at 25 °C	0.91
Viscosity/mm <sup>2</sup> s <sup>-1</sup> at 38 °C	39.98
Acid value	3.62
Iodine value (I <sub>2</sub> g 100 g <sup>-1</sup> )	59.5
Saponification value/mg KOH g <sup>-1</sup>	190
Peroxide value/meq O <sub>2</sub> kg <sup>-1</sup>	12.15
Water content/mass%	0.037
Fatty acid composition/%	
Palmitic (C16:0)	5.4
Stearic (C18:0)	35.7
Oleic (C18:1)	49.6
Linoleic (C18:2)	7.8
Arachidic (C20:0)	1.3

precision and well-controlled experimental conditions [15–17]. Several researchers investigated the use of TG for evaluation of biomass kinetic parameters [18, 19]. Likewise, various models have been used varying the heating rates to avoid confusion that may arise from single heating rate [1]. Therefore, it is needful to study pyrolysis of shea butter and the produced biodiesel under non-isothermal thermogravimetric condition to have a better understanding of their kinetic analysis as well as stability. This will give insight into the biodiesel production process.

This study investigates the thermal behavior and pyrolysis kinetics of shea butter and its biodiesel samples by thermogravimetric analysis. The kinetic triplets were computed with the aid of the experimental data using Coats–Redfern, Ingraham–Marrier, Arrhenius and Differential model. The degradation kinetics was performed to investigate the effect of different catalysts on activation energy and frequency factor.

## Experimental

### Materials and methods

Crude shea butter was procured from Lagos, Nigeria. The biodiesel samples were synthesized over conventional ZSM-5 and desilicated ZSM-5 as described in our previous work [3]. Two samples of desilicated ZSM-5 were used (0.3HZSM-5 and 0.4HZSM-5). The biodiesel produced from ZSM-5, 0.3HZSM-5 and 0.4HZSM-5 is designated ZBio, 0.3mesoZBio and 0.4mesoZBio, respectively, at 200 °C for 18 h using 5:1 methanol/oil ratio according to our previous work [3].

Determination of higher heating value (HHV) was done using an oxygen bomb calorimeter (Parr 6100) according to ASTM M240 (2009). Anton Paar density meter (DMA 4500M USA) and Brookfield (USA) DV-E viscometer were used for density and viscosity measurement, respectively. Further, the elemental composition was determined using Perkin Elmer 2400 Series II CHNS analyzer (Perkin Elmer SdnBhd, Selangor, Malaysia).

The shea butter and biodiesel samples were pyrolyzed using TA Q60. The analysis proceeds in the presence of nitrogen at a constant heating rate from 293.15 until 550 °C. Multiple heating rates of 10, 15 and 20 °C min<sup>-1</sup> were used according to ICTAC Kinetics committee recommendations for kinetic computations on thermal analysis data [14]. The nitrogen flow helped to maintain inert atmosphere to avoid unwanted oxidation.

### Determination of kinetic parameters

Due to numerous reactions in both series and parallel, kinetic study of pyrolysis process is a complex process. Generally, the decomposition rate is given by

$$\frac{dx}{dt} = K(T)f(x)^n \quad (1)$$

where  $x$  is the degree of conversion,  $T$  is temperature and  $t$  is time. The conversion rate  $\frac{dx}{dt}$  for pyrolysis at constant heating rate,  $\beta = \frac{dT}{dt}$ , could be written as;

$$\frac{dx}{dt} = \beta \frac{dx}{dT} = K(T)f(x) \quad (2)$$

Also, the degree of advance,  $x$  is:

$$x = \frac{w_0 - w}{w_0 - w_f} \quad (3)$$

where  $w_0$ ,  $w_f$  and  $w$  refer to mass of samples at the beginning, end and time,  $t$ , respectively. Since mass loss is temperature dependent,  $K(T)$  is often modeled by Arrhenius equation [20].

$$K(T) = A \exp\left(-\frac{E_A}{RT}\right) \quad (4)$$

where  $R$  is the gas constant (8.314 J mol<sup>-1</sup> K<sup>-1</sup>),  $A$  is the frequency factor, min<sup>-1</sup>,  $E_A$  is the activation energy, kJ mol<sup>-1</sup> and  $T$  is the absolute temperature,  $K$ . Combination of Eqs. (1) and (2) gives:

$$\beta \frac{dx}{dT} = A \exp\left(-\frac{E_A}{RT}\right)f(x) \quad (5)$$

To analyze the TG data, kinetic models are employed. Coats–Redfern, Ingraham–Marrier, Arrhenius and Differential model are used.

Arrhenius model suggests that the total rate of decomposition depends on temperature, sample mass remaining and rate constant. Therefore, Eq. (5) becomes:

$$\log \left[ \frac{dw}{dt} \right] = \log A - (E_A/2.303RT) \quad (6)$$

Plotting  $\log[dW/dt/w]$  versus  $1/T$  gives a linear plot whose slope corresponds to  $-E_A/2.303R$  and the intercept gives  $\log A$ . This gives the value of activation energy and frequency factor.

The integral model developed by Coats and Redfern [9] suggests that the correct order leads to the best straight-line plot. Therefore, Eq. (5) becomes:

$$\ln \left( \frac{g(x)}{T^2} \right) = \ln \left( \frac{AR}{\beta E_A} \right) - E_A/(RT) \quad (7)$$

Plotting  $\ln(g(x)/T^2)$  versus  $1/T$  results in a linear plot whose slope corresponds to  $-E_A/R$  and the intercept gives  $\ln(AR/\beta E_A)$ . This gives the value of activation energy and Arrhenius constant/frequency factor. Table 1 gives the values of the function  $g(x)$ .

Ingraham and Marrier [21] expressed rate constant  $K$  as  $dw/dt$  for the linear kinetics of the heterogeneous reaction, where  $dw$  is the mass loss per unit area at  $dt$  period. Therefore, Eq. (5) becomes:

$$\log \left( \frac{dw}{dT} \right) = -\log T - \log \beta + \log A - E_A/(2.303RT) \quad (8)$$

The graph of  $\log(dw/dT) + \log T + \log \beta$  versus  $1/T$  offers a linear plot whose slope corresponds to  $-E_A/2.303R$  and the intercept gives  $\log A$ . This gives the value of activation energy and Arrhenius constant/frequency factor.

Differential model combines Eqs. (1) and (4) to give [22, 23]:

$$\ln \left( \left( \frac{dx}{dt} \right) / f(x) \right) = \ln A - E_A/(RT) \quad (9)$$

The graph of  $\ln((dx/dt)/f(x))$  versus  $1/T$  offers a linear plot whose slope corresponds to  $-E_A/R$  and the intercept gives  $\ln A$ . This gives the value of activation energy and Arrhenius constant/frequency factor. Table 2 gives the values of the function  $f(x)$ .

## Result and discussion

### Physicochemical properties of shea butter and biodiesel samples

Table 3 presents the physicochemical properties of shea butter and biodiesel samples. The biodiesel yield is between 83 and 87 %, and the density reduced upon transesterification. The biodiesel samples also exhibit high heating value (HHV) of 39.98–40.10 MJ kg<sup>-1</sup>.

### TG pyrolysis of shea butter and biodiesel samples

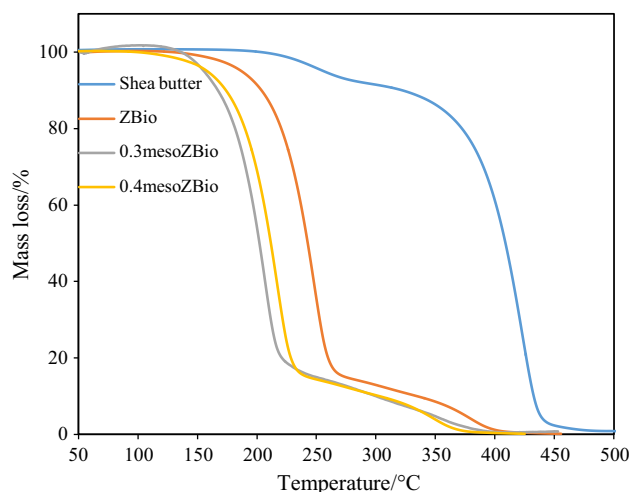
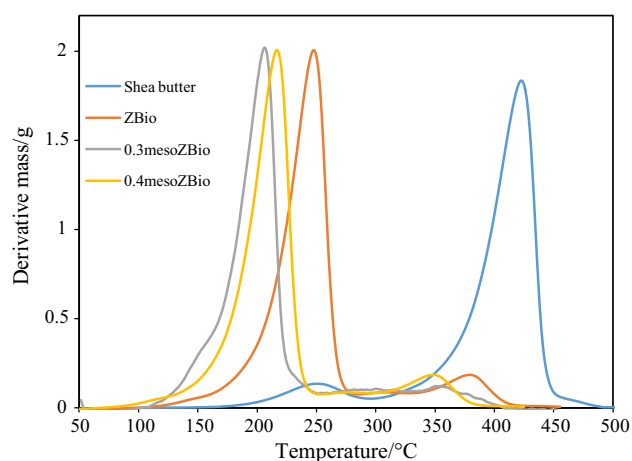
Figures 1 and 2 present the TG and DTG curve for shea butter and biodiesel samples. Decomposition of shea butter proceeds in two steps as evident in DTG curve with a small peak and a long one. The former corresponds to breakage of unsaturated/bulky triglyceride molecules, while the latter corresponds to the total decomposition of the shea butter. Moreover, biodiesel decomposition proceeds in two steps, as evident in the DTG curve with two peaks. The first peak shows total devolatilization of methyl ester, while the other is for decomposition of glycerol and unconverted shea butter. Figure 3 gives the DTG decomposition characteristics of shea butter and those of biodiesel samples. The sample DTG peak temperature shown is a measure of its stability. The sample stability is in the order of shea butter > ZBio > 0.4mesoZBio > 0.3mesoZBio. Generally, the increase in heating rate delays the peak temperature. However, for the produced biodiesel samples, only

**Table 2** Algebraic expressions of functions of the most common reaction mechanism

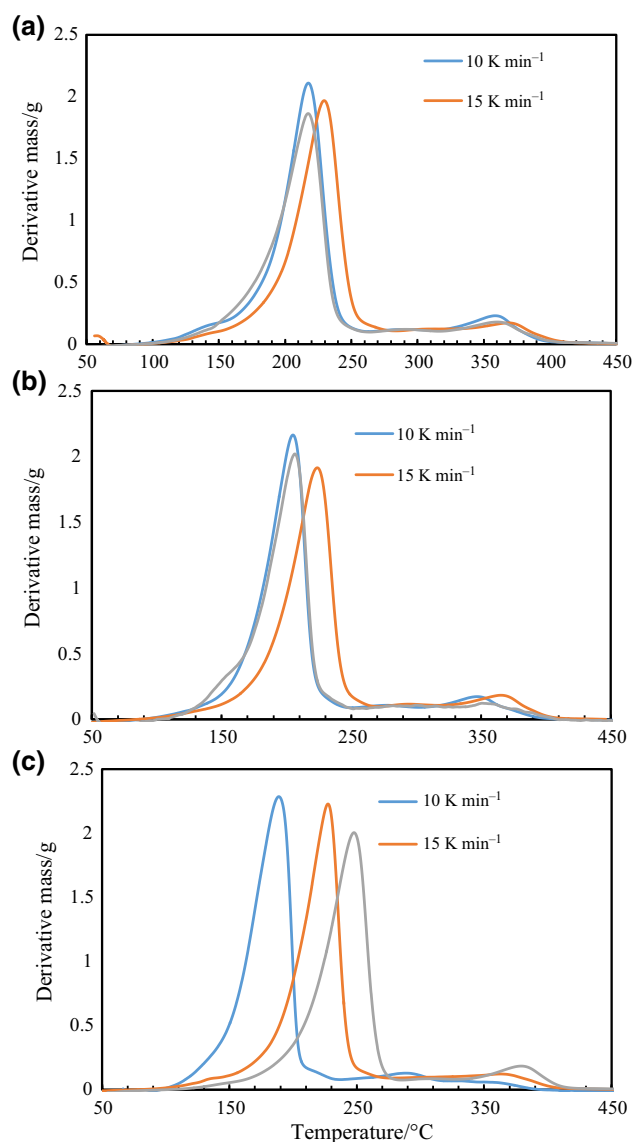
Mechanism	$f(x)$	$g(x)$
Power law	$2x^{1/2}$	$x^{1/2}$
Power law	$3x^{2/3}$	$x^{1/3}$
Power law	$4x^{3/4}$	$x^{1/4}$
One-dimensional diffusion model	$1/2x$	$x^2$
Two-dimensional diffusion model	$[-\ln(1-x)]^{-1}$	$[(1-x)\ln(1-x)] + x$
Three-dimensional diffusion model	$3(1-x)^{2/3}/[2(1-(1-x)^{1/3})]$	$1 - (2x/3) - (1-x)^{2/3}$
First-order reaction model	$(1-x)$	$-\ln(1-x)$
Second-order reaction model	$(1-x)^2$	$(1-x)^{-1} - 1$
Third-order reaction model	$(1-x)^3$	$[(1-x)^{-2} - 1]/2$

**Table 3** Properties of crude shea butter and biodiesel samples

Properties	Values			
	Shea butter	ZBio	0.3mesoZBio	0.4mesoZBio
Biodiesel yield/%	—	86.17	82.82	83.36
Density/kg m <sup>-3</sup> at 25 °C	0.91	0.85	0.87	0.86
Viscosity/mm <sup>2</sup> s <sup>-1</sup> at 38 °C	39.98	3.35	3.38	3.36
HHV/MJ kg <sup>-1</sup>	—	40.05	39.98	40.10
Carbon	77.82	76.33	76.85	76.38
Hydrogen	12.79	12.82	12.80	12.95
Oxygen	9.304	9.77	10.26	9.79

**Fig. 1** TG curves of shea butter and biodiesel samples**Fig. 2** DTG curves of shea butter and biodiesel samples

ZBio complies with the trend. 0.4mesoZBio and 0.3mesoZBio exhibit quite unusual trend as the heating rate was increased to 20 °C min<sup>-1</sup>. This trend is concomitant with the findings of Song et al. [24] regarding kinetics of reed black liquor (RBL) pyrolysis from TG/DTG data.

**Fig. 3** DTG curves of biodiesel samples at varying heating rate. **a** 0.4mesoZBio, **b** 0.3mesoZBio and **c** ZBio

### Kinetics analysis

The reaction models for shea butter and biodiesel samples were developed from TG data with the aid of Microsoft Excel spreadsheet. The reaction region used is the most linear region of the TG curve. The slopes and intercept of the linear curves were used for computation of corresponding  $E_A$  and  $A$  values as presented in Tables 4 and 5, respectively. Variation in the  $E_A$  and  $A$  values with respect to different kinetic models is mainly because the models are developed with different parameters and different assumptions. The first reaction region of shea butter follows third-order process with lower  $E_A$  (91.17 kJ mol<sup>-1</sup>) value, while the second region follows first order with high  $E_A$  (115.82 kJ mol<sup>-1</sup>).

From the assessment of the average  $E_A$  values of the samples, the  $E_A$  value is in the order of shea butter > ZBio > 0.3mesoZBio > 0.4mesoZBio (Table 6). This shows that shea butter is more stable than biodiesel samples. It also authenticates the effect of transesterification process on shea butter. Moreover, among the biodiesel samples, ZBio is the most stable, while 0.4mesoZBio is the least stable since stability decreases with a decrease in  $E_A$  [25]. Therefore, more heat is required to oxidize ZBio sample than 0.3mesoZBio and 0.4mesoZBio. Further, the high  $E_A$  value of ZBio is maybe due to higher acidity of ZSM-5 used compared to the desilicated ZSM-5 used for 0.3mesoZBio and 0.4mesoZBio. This shows that  $E_A$  may be a direct function of catalyst acidity.

**Table 4** TG/DTG Activation energies ( $E_A$ /kJ mol<sup>-1</sup>) of shea butter and biodiesel samples

Sample	$\beta/^\circ\text{C min}^{-1}$	Arrhenius	Coast–R. $n = 1$	Ingraham–M.	Diff. $n = 1$
ZBio	10	57.64	95.46	61.36	102.38
	15	69.11	101.50	61.05	123.38
	20	68.48	102.80	72.70	122.54
0.3mesoZBio	10	54.14	122.83	56.14	137.61
	15	49.28	89.33	80.02	107.83
	20	56.08	101.30	56.68	92.08
0.4mesoZBio	10	67.67	105.39	69.15	119.72
	15	76.63	93.79	80.65	87.71
	20	67.21	92.14	70.52	107.49
Shea butter					
Region 1	20	75.83	102.10, $n = 3$	79.84	76.92, $n = 3$
Region 2	20	115.39	77.24	120.79	149.88

C–R. Coats–Redfern,  $P(I)$  Power law 1,  $I$ –M. Ingraham–Marrier,  $Diff.$  Differential

**Table 5** TG/DTG Arrhenius,  $A/\text{min}^{-1}$  of shea butter and biodiesel samples

Sample	$\beta/^\circ\text{C min}^{-1}$	Arrhenius	Coast–R. $n = 1$	Ingraham–M.	Diff. $n = 1$
ZBio	10	5.05E+06	6.39E+07	2.05E+10	1.02E+02
	15	6.22E+06	3.52E+07	1.50E+09	1.03E+11
	20	1.68E+06	1.03E+08	2.19E+10	1.09E+12
0.3mesoZBio	10	4.99E+05	1.22E+08	2.97E+09	2.22E+15
	15	1.42E+05	1.84E+06	3.96E+11	2.34E+11
	20	1.68E+06	8.39E+10	1.53E+09	3.14E+10
0.4mesoZBio	10	5.94E+06	1.54E+08	4.07E+10	1.22E+13
	15	3.40E+07	3.87E+06	3.30E+11	6.39E+08
	20	1.29E+07	4.74E+06	3.33E+10	5.16E+11
Shea butter					
Region 1	20	1.34E+06	9.25E+08, $n = 3$	9.13E+09	1.80E+06, $n = 3$
Region 2	20	1.78E+05	2.16E+05	1.63E+12	1.57E+11

C–R. Coats–Redfern,  $P(I)$  Power law 1,  $I$ –M. Ingraham–Marrier,  $Diff.$  Differential

**Table 6** Average activation energies

Sample	$\beta/^\circ\text{C min}^{-1}$	$E_A/\text{kJ mol}^{-1}$	Average $E_A/\text{kJ mol}^{-1}$
ZBio	10	79.21	86.53
	15	88.76	
	20	91.63	
0.3mesoZBio	10	92.68	83.61
	15	81.62	
	20	76.53	
0.4mesoZBio	10	80.74	83.26
	15	84.70	
	20	84.34	
Shea butter			
Region 1	20	91.17	91.17
Region 2	20	115.82	115.82

## Conclusions

The thermal degradation of the shea butter and the biodiesel samples was investigated at different heating rates in the presence of  $\text{N}_2$ . The activation energy is in the order of shea butter > ZBio > 0.3mesoZBio > 0.4mesoZBio because the microporous ZSM-5 zeolites used for ZBio exhibits higher acidity. This shows that more heat is required to oxidize ZBio than for the other samples. However, the high conversion was also achieved over both 0.3mesoZBio and 0.4mesoZBio due to the combination of mesopore advantages. This shows that pyrolysis kinetics and reaction of the produced biodiesel depend on acidity and porosity of the catalyst as well as the heating rate.

**Acknowledgements** This study was carried out with the aid of a research grant from Fundamental Research Grant Scheme (FRGS) Grant (Project No.: FP031-2013A) under University of Malaya.

## References

1. Biswas S, Sharma D. Studies on cracking of jatropha oil. *J Anal Appl Pyrol.* 2013;99:122–9.
2. Ounas A, Aboulkas A, Bacaoui A, Yaacoubi A. Pyrolysis of olive residue and sugar cane bagasse: Non-isothermal thermogravimetric kinetic analysis. *Bioresour Technol.* 2011;102:11234–8.
3. Alaba PA, Sani YM, Mohammed IY, Abakr YA, Daud WMAW. Synthesis and application of hierarchical mesoporous HZSM-5 for biodiesel production from shea butter. *J Taiwan Inst Chem Eng.* 2016;59:405–12.
4. Jasaw GS, Saito O, Takeuchi K. Shea (*Vitellaria paradoxa*) butter production and resource use by urban and rural processors in northern ghana. *Sustainability.* 2015;7:3592–614.
5. Enweremadu C, Rutto H, Oladeji J. Investigation of the relationship between some basic flow properties of shea butter biodiesel and their blends with diesel fuel. *Int J Phys Sci.* 2011;6:758–67.
6. Betiku E, Okunsolawo SS, Ajala SO, Odedele OS. Performance evaluation of artificial neural network coupled with generic algorithm and response surface methodology in modeling and optimization of biodiesel production process parameters from shea tree (*Vitellaria paradoxa*) nut butter. *Renew Energy.* 2015;76:408–17.
7. Enweremadu CC, Rutto HL, Peleowo N. Performance evaluation of a diesel engine fueled with methyl ester of shea butter. *World Acad Sci Eng Technol.* 2011;79:142–6.
8. Sait HH, Hussain A, Salema AA, Ani FN. Pyrolysis and combustion kinetics of date palm biomass using thermogravimetric analysis. *Bioresour Technol.* 2012;118:382–9.
9. Apaydin-Varol E, Polat S, Putun AE. Pyrolysis kinetics and thermal decomposition behavior of polycarbonate—a TGA-FTIR study. *Therm Sci.* 2014;18:833–42.
10. Abnisa F, Wan Daud W, Arami-Niya A, Ali BS, Sahu J. Recovery of liquid fuel from the aqueous phase of pyrolysis oil using catalytic conversion. *Energy Fuels.* 2014;28:3074–85.
11. Abnisa F, Daud WMAW. A review on co-pyrolysis of biomass: an optional technique to obtain a high-grade pyrolysis oil. *Energy Convers Manag.* 2014;87:71–85.
12. Rutkowski P, Kata D, Jankowski K, Piekarczyk W. Thermal properties of hot-pressed aluminums nitride-graphene composites. *J Thermal Anal Calorim.* 2016;124:93–100.
13. Ciecierska E, Jurczyk-Kowalska M, Bazarnik P, Kowalski M, Krauze S, Lewandowska M. The influence of carbon fillers on the thermal properties of polyurethane foam. *J Therm Anal Calorim.* 2016;123:283–91.
14. Szumera M, Waclawska I, Sułowska J. Thermal properties of  $\text{MnO}_2$  and  $\text{SiO}_2$  containing phosphate glasses. *J Therm Anal Calorim.* 2016;123:1083–9.
15. Wicinska P. Thermal degradation of organic additives used in colloidal shaping of ceramics investigated by the coupled dta/tg/ms analysis. *J Therm Anal Calorim.* 2016;123:1419–30.
16. Szczygiel I, Winiarska K. Synthesis and characterization of manganese-zinc ferrite obtained by thermal decomposition from organic precursors. *J Therm Anal Calorim.* 2014;115:471–7.
17. Sułowska J, Waclawska I, Szumera M. Comparative study of zinc addition effect on thermal properties of silicate and phosphate glasses. *J Therm Anal Calorim.* 2016;123:1091–8.
18. Ksepko E, Babinski P, Evdou A, Nalbandian L. Studies on the redox reaction kinetics of selected, naturally occurring oxygen carrier. *J Thermal Anal Calorim.* 2016;124:137–50.
19. Ksepko E, Sciazko M, Babinski P. Studies on the redox reaction kinetics of  $\text{Fe}_2\text{O}_3$ - $\text{CuO}/\text{Al}_2\text{O}_3$  and  $\text{Fe}_2\text{O}_3/\text{TiO}_2$  oxygen carriers. *Appl Energy.* 2014;115:374–83.
20. Aboulkas A, Nadifiyine M, Benchanaa M, Mokhlisse A. Pyrolysis kinetics of olive residue/plastic mixtures by non-isothermal thermogravimetry. *Fuel Process Technol.* 2009;90:722–8.
21. Kök MV, Pamir MR. Comparative pyrolysis and combustion kinetics of oil shales. *J Anal Appl Pyrol.* 2000;55:185–94.
22. Aboulkas A, El Harfi K, El Bouadili A, Benchanaa M, Mokhlisse A, Outzourit A. Kinetics of co-pyrolysis of tarfaya (morocco) oil shale with high-density polyethylene. *Oil Shale.* 2007;24:15–33.
23. Dollimore D. The application of thermal analysis in studying the thermal decomposition of solids. *Thermochim Acta.* 1992;203:7–23.
24. Song X, Bie R, Ji X, Chen P, Zhang Y, Fan J. Kinetics of reed black liquor (rbl) pyrolysis from thermogravimetric data. *BioResources.* 2014;10:137–44.
25. Souza A, Danta H, Silva MC, Santos IM, Fernandes V, Sinfrônio FS, Teixeira LS, Novák C. Thermal and kinetic evaluation of cotton oil biodiesel. *J Therm Anal Calorim.* 2007;90:945–9.